MAGNETIC RESONANCE IN CHEMISTRY
Magn. Reson. Chem. **36**, 693–705 (1998)

High-field NMR spectroscopic techniques combined with molecular dynamics simulations for the study of the inclusion complexes of α- and β-cyclodextrins with the cognition activator 3-phenoxypyridine sulphate (CI-844)

Maria E. Amato,[1] Kenny B. Lipkowitz,[2] Giuseppe M. Lombardo[3] and Giuseppe C. Pappalardo[3]*

[1] Dipartimento di Scienze Chimiche, Università di Catania, Viale A. Doria 6, 95125 Catania, Italy
[2] Department of Chemistry, Indiana University–Purdue University at Indianapolis, Indianapolis, Indiana 46202, USA
[3] Dipartimento Di Scienze Chimiche, Cattedra di Chimica Generale, Facoltà di Farmacia, Università di Catania, Viale A. Doria 6, 95125 Catania, Italy

Received 19 December 1997; revised 1 April 1998; accepted 6 April 1998

ABSTRACT: The formation of complexes and the mode of binding to macrocyclic host molecules (α- and β-cyclodextrins, CDs) of the nootropic drug CI-844 (3-phenoxypyridine sulphate, Warner-Lambert/Parke-Davis) were studied using NMR techniques (T-ROESY) complemented by molecular dynamics (MD) protocols which allowed complete interpretation of the NMR experimental data. The NMR experiments indicated that a 1:1 stoichiometry of the complexes exists and revealed dipolar contacts between selected protons of the guest and inner protons of the hosts. The NMR data suggest the same relative host–guest alignment in the complexes, but that the guest has different mobilities in the complexes formed. The MD simulations in the gas phase gave a first rough indication of the structure of each complex. The MD simulations with explicit water molecules reproduced the experimental sets of ^{1}H–^{1}H contacts and thus provided reliable information on the relative host–guest alignments and geometries of the complexes. In the β-Cd complex the CI-844 molecule penetrates deeply into the cavity from the larger rim side with the phenyl-group moiety. An analogous relative host–guest alignment as in the β-CD complex was found in the α-CD complex. In this latter case the CI-844 is not deeply embedded into the host's cavity, and the guest fluctuates widely about the equilibrium position, thus denoting lower stability of the α-CD–CI-844 complex with respect to the β-CD–CI-844 complex. The use of β-CD as host is therefore adequate for vehiculation of the drug. The relative hydrophobic–hydrophilic energetics of the phenyl and pyridinium rings of CI-844 were the factor determining the orientation of the guest in the inclusion process. The study also confirmed the importance of including explicitly the solvent molecules in the simulations of ionic systems in order to interpret correctly the experimental data and the location of the host–guest contact distances falling within 3.5 Å (NOE effective) and their fluctuations. © 1998 John Wiley & Sons Ltd.

KEYWORDS: NMR; inclusion complexes; cyclodextrin; ROESY; molecular dynamics

INTRODUCTION

Cyclodextrins (CDs) are cyclic oligomers of $1 \rightarrow 4$-linked α-D-glucose monomers. Because of this topology, the CDs as a class of macromolecules, in both their native and derivatized forms, possess a relatively hydrophobic cavity. In turn, they can recognize and form inclusion complexes in water solution with an astonishingly wide variety of organic and inorganic molecules.[1,2] The stability of CD complexes in solution has recently been reviewed.[3] Moreover, because they are easily modified, they can be adapted to provide advantageous properties of complexed substances such as increased solubility, bioavailability and stability, and for this reason they have become important molecular encapsulators of drugs.[4]

* Correspondence to: G. C. Pappalardo, Dipartimento di Scienze Chimiche, Cattedra di Chimica Generale, Facoltà di Farmacia, Università di Catania, Viale A. Doria 6, 95125 Catania, Italy.
E-mail: gcpappalardo@dipchi.unict.it

Recent research endeavours in the field of medicinal chemistry have been focused on 'nootropics', which are new drugs for the treatment of cognitive disorders and age-related brain syndromes.[5,6] The pharmaceutical importance of 3-phenoxypyridine sulphate (CI-844) stems from its activity as a cognition activator.[7,8] Both the simple chemical structure and the activity of this drug appear as important arguments for its clinical use which may be favoured by controlled release and by increased bioavailability. Therefore, preliminary studies on the formation of supramolecular assemblies of CI-844 with CDs seemed in order for future assessment of vehiculation techniques suited for its administration.

The major impediment to our understanding of the structural features of CD host–guest complexes is the shortcoming of classical NOE–NMR experiments in solution ($\omega\tau_c \approx 1$) and, when in the solid state, they are materials of low crystallinity or more usually amorphous, thus making traditional x-ray diffraction analysis difficult or otherwise impossible. Moreover, because of NMR time-scales, only the time-average structure is

 CCC 0749-1581/98/100693–13 $17.50

derived so instantaneous information concerning the dynamics of structural changes is not easily derived and much of the information from, say, intermolecular NOE data is ambiguous. In that regard one of the more significant shortcomings of NMR spectroscopy involves its inability to describe the regioselection of host–guest binding, i.e. whether the guest is inserted into the cavity 'head-first' or in a reversed orientation. To supplement these experimental investigations many workers have relied on computational chemistry, as reviewed recently.[9] Their goal is to apply adequately experimental and theoretical computational tools capable of providing the structural, energetic, binding mechanisms and dynamic features of CD complexes.

Several approaches are commonly used to determine the geometry of such complexes in solution, including 1D- and 2D-NMR experiments. While ^{1}H and ^{13}C chemical shifts provide unambiguous evidence on the formation of the complex, relaxation times and NOE or ROE experiments have been demonstrated to provide information on the dynamics and the averaged relative inter- and intramolecular proton distances, respectively.[10–12] The NMR data are typically analysed in terms of structures based on molecular mechanics force field calculations, using geometry optimization of static models.[11] The inherent limitations of this approach are well known, especially the fact that one is not ensemble averaging and, accordingly, making comparisons with experiment can become meaningless, especially for the highly mobile complexes as they exist in solution. One can overcome this deficiency, though, by implementing a technique that ensemble averages such as Monte Carlo (MC) or molecular dynamics (MD) techniques so that direct comparison with experimental data is possible. Because workers often want dynamic information, the more appropriate MD simulation techniques[13,14] are used. With currently available high-speed workstations and the associated software, the MD scheme is becoming the technique of choice for deriving atomic level insights into the structures, energetics, dynamics, reactivity and properties of complex molecular systems in their effective environment. In particular, MD techniques have the ability (i) to monitor the internal molecular fluctuations, (ii) to generate microscopic-level information that can be correlated directly with experimentally detectable macroscopic properties, (iii) to investigate diffusional aspects of the inclusion process and (iv) to help refine molecular structures using experimental data, especially x-ray diffraction data for crystalline and amorphous solid phases, and NMR data such as NOE intensities, relaxation times and coupling constants in the liquid phase.

Accurate elucidation of supramolecular structures such as those of CD inclusion complexes can thus be derived from molecular simulation. Those data must be consistent with the experimental NMR data, however, to ensure a coherent argument; when the MD and NMR data are consonant, the MD model can be used to describe details of the structural, energetic and dynamic features of the host–guest complex that are otherwise inaccessible from experiment alone. Because of these distinct advantages, we have been utilizing MD simulations as a technique complementary to our NMR experimental programme. The application of MD techniques for modelling the structure and dynamics of complexes in solution is limited, especially compared with the number of molecular mechanics calculations that have been published.[9]

Accordingly, in this work we primarily focused on the formation and stability of the supramolecular aggregates formed by CI-844 with both α- and β-CD. For this purpose NMR T-ROESY experiments were combined with MD simulations.

In the course of this study, the MD runs were initiated from several different host–guest relative alignments and positioning. This compensates for the fact that we are generally unable to explore fully all of phase space arising, in part, from high energy barriers that cannot be overcome during the simulation time period. Hence the MD results are expected to depend on the imposed initial conditions. By randomly placing the guest molecule on the host–guest hypersurface we are intentionally exploring other regions of phase space.

Our recent study[15] showed that solvation effects selectively control the formation of complexes of β-CD with charged species. Therefore, in the present study, MD simulations explicitly including water molecules were performed.

Scheme 1 shows the labeling scheme of CDs and CI-844.

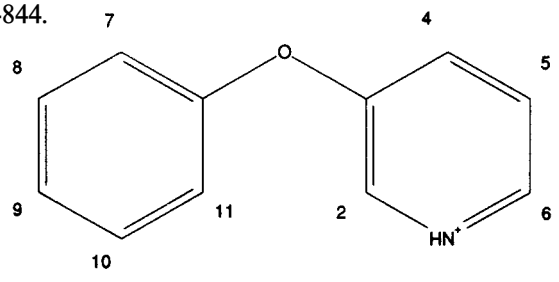

CI-844

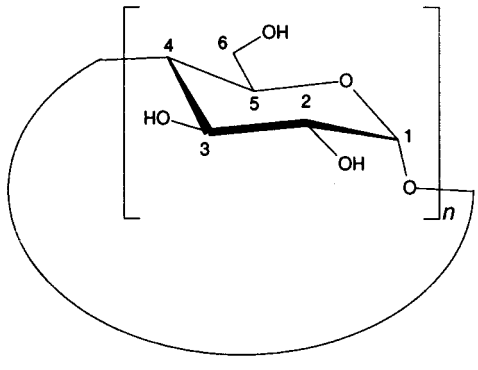

α-CD (*n*=6); β-CD (*n*=7)

Scheme 1

The combined approach thus allowed us to achieve unique insights into features such as structure, geometry and internal fluctuations of the supramolecular assemblies, and also to monitor hydrophobic–hydrophilic energetics determining the inclusion and the host–guest relative alignments.

EXPERIMENTAL

Materials

The sample of CI-844 [3-phenoxypyridine sulphate, $(C_{11}H_{10}NO)^+$ $(HSO_4)^-$] was a gift from Warner-Lambert/Parke-Davis, Ann Arbor, MI, USA). The α- and β-CDs (Fluka, Buchs, Switzerland) were used as received.

The samples for complexation studies were prepared by mixing suitable volumes of stock solutions (10 mmol dm^{-3}) in D_2O of guest and CDs.

NMR spectroscopy

The ^1H NMR experiments were performed at 499.89 MHz on a Varian Unity Inova 500 spectrometer. The probe temperature was regulated at 300 ± 0.1 K. The chemical shifts were measured relative to external TSP. The stoichiometry and formation constants of the complexes were determined using the continuous variation[16] and Benesi–Hildebrand[17] methods, respectively. The T-ROESY experiments[18] (software supplied by Varian) were performed in phase-sensitive mode using the hypercomplex method with $2 \times 256t_1$ increments. The conditions were as follows: spectral widths, 10 ppm with 2048 complex points in F_2; mixing time, 1 s; spin lock field, 2000 Hz; 16 scans; and presaturation of residual HDO signal during relaxation delay (1.8 s). The data were processed with zero filling to 1024 in F_1 and a non-shifted sine-bell window in both dimensions. The relaxation times were measured using the inversion–recovery pulse sequence.[19]

Molecular dynamics simulations

Protocols. MD calculations were performed using the CHARMm program[20] (version 2.4g1). All the simulations in this study used the SHAKE algorithm (on the bonded hydrogen atoms) and the constant temperature (CPT CHARMm command) algorithm. The system was kept at 298 K with a thermal bath coupling constant of 5.0 ps. The integration time step and non-bond cut-off radius were 0.002 ps and 15 Å, respectively.

Transients for 500 ps (2.5×10^5 steps) with a sampling interval of 0.5 ps (at every 250 steps) were usually collected in all simulations.

The preliminary minimizations which produced the starting structures for dynamics were performed using the ABNR (Adopted Basis Newton–Raphson) algorithm up to a gradient of 0.01 kcal mol^{-1} $Å^{-1}$ (1 kcal = 4.184 kJ).

Models. The input coordinates for structure minimizations of the isolated supramolecule came from the x-ray structures of the guest,[21] α-CD,[22] and β-CD.[23,24] The extraneous atoms were deleted. The total charge for the CI-844 was set to + 1. The atomic charges for each atom of CI-844 were set at the values* obtained by fitting the MEP[25] (molecular electrostatic potential) calculated using the MNDO[26] method. The atomic charges for CDs were those included in the CHARMm database.

The starting structures were built by accommodating the guest into the host with the molecules aligned along their principal inertial axes in the two possible relative orientations **I** and **II** as shown in Fig. 1. The centres of mass (CMs) of the host and of the guest were set at various distances (d) along the symmetry axis of the torus as depicted in the Fig. 1. All the simulations of the α- and β-CD complexes with CI-844 were performed starting from the above arrangements for each complex.

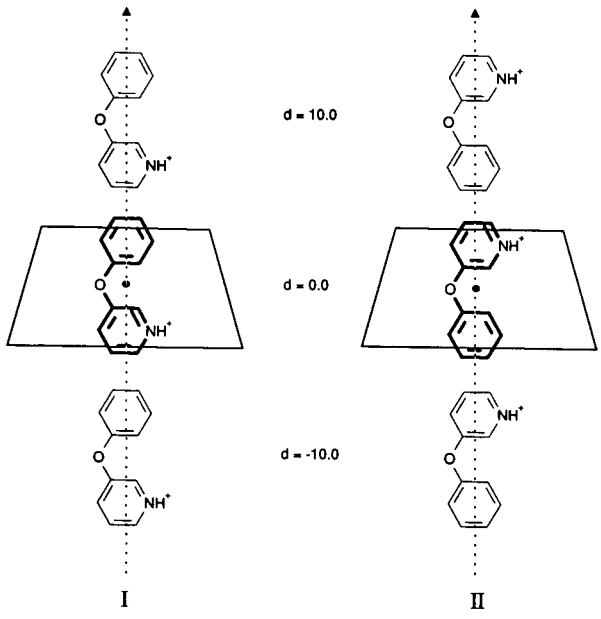

Figure 1. Alignment scheme and relative orientations (**I** and **II**) of the host and guest molecules. The alignment is made along the principal inertial axes of CI-844 and the CD. The positioning of the centre of mass (CM) of the guest at the various distances d (Å) from the origin in the starting structures for MD simulations of orientations **I** and **II** is outlined. The origin is assumed at the CM of the CD (marked by ●), and the symmetry axis of the CD torus is chosen as displacement vector (positive direction denoted by dotted arrow). The CMs coincide at positioning $d = 0.0$ Å.

* O, −0.1829; N, −0.0996; H(N), 0.2510; C-1, 0.1486; C-2, 0.0703; C-4, 0.0010; C-5, −0.0463; C-6, 0.0915; C-7, −0.0427; C-8, −0.0425; C-9, −0.0214; C-10, −0.0425; C-11, −0.0427; H-2, 0.1520; H-4, 0.1229; H-5, 0.1250; H-6, 0.1404; H-7, 0.0782; H-8, 0.0841; H-9, 0.0856; H-10, 0.0841; H-11, 0.0782.

The complexes were simulated using both gas-phase and water sphere models. In the gas-phase MD simulations the effect of the medium was mimicked using a distance-dependent dielectric constant ($\varepsilon = R$ in gas; $\varepsilon = 1$ in liquid phase).

The MD simulations in solution were performed by including explicitly water molecules in the model. The three interaction sites TIP3P water model of the CHARMm package was used for the MD runs. Every complex was immersed in the water sphere of diameter 30 Å containing 464 H_2O molecules (density 1 g cm^{-3}). The water molecules within a distance of 2.8 Å around the complex were removed to avoid overlapping between solute and solvent molecules.

A stochastic boundary constraint (SBOUnd routine) to keep the water molecules within the sphere was applied to every MD evolution.[27]

RESULTS AND DISCUSSION

NMR data

The ^{1}H NMR spectrum of the pure CI-844 was reported previously.[21] The existence of dimers or larger aggregates of CI-844 in solution was excluded on the basis of the absence of concentration-dependent ^{1}H chemical shifts. The formation of inclusion complexes with α- and β-CD in the fast exchanging regime on the NMR time-scale was evidenced by the observed characteristic upfield shifts of the inner cavity ^{1}H resonances compared with those of solutions of the pure macrocycles (Table 1).

Table 1 shows that in the case of the β-CD complex, the upfield shifts of H-3 and H-5 resonances are significantly larger than those of the α-CD complex. In both complexes, the resonances of the methylenic H-6 are shifted relatively much less upfield with respect to H-3 and H-5, and the outer H-1, H-2 and H-4 nuclei of the macrocycles were almost unaffected by the complexation.

This can be reasonably accounted for by the different structures of the complexes, since the larger radius of the β-CD ring allows a deeper accommodation of the embedded aromatic ring.

Table 1 shows that all guest hydrogen resonances are appreciably deshielded in the case of the β-CD complex (with the exception of H-4, which was shifted slightly upfield). This feature can be attributed to a dielectric change of the environment surrounding the aromatic ring, imposed by inclusion inside the hydrophobic macrocycle cavity. In contrast, very small (minimal) variations of the CI-844 proton chemical shifts were observed for the α-CD complex. Information derived from these changes could not support adequately any speculative hypothesis on the most probable average structure of the complexes in solution.

Table 1. Chemical shifts (δ_{free}), the corresponding variation ($\Delta\delta$) due to the complexation and ^{1}H spin–lattice relaxation times of free guest and hosts, and of CD–CI-844 complexes (solution concentration of host and guest 5 mmol dm^{-3})

		Free		α-CD–CI-844 complex		β-CD–CI-844 complex	
Species		δ_{free} (ppm)	T_1 [b] (s)	$\Delta\delta$[a] (ppm)	T_1 [b] (s)	$\Delta\delta$[a] (ppm)	T_1 [b] (s)
CI-844	H-2	8.413	10.075	0.004	7.316	−0.063	6.318
	H-4	8.077	6.309	0.004	4.86	0.024	3.758
	H-5	7.908	5.279	0.023	4.104	−0.042	3.545
	H-6	8.408	10.075	0.018	6.498	−0.05	5.55
	H-7,11	7.157	7.111	−0.01	4.130	−0.043	3.476
	H-9	7.305	6.515	−0.017	3.675	−0.037	3.299
	H-8,10	7.461	5.774	−0.002	3.649	−0.046	2.996
α-CD	H-1	5.02	0.88	0.001	0.89		
	H-2	3.6	1.45	0.01	1.42		
	H-3	3.95	1.25	0.045	1.12		
	H-4	3.55	0.85	0.01	0.81		
	H-5	3.81	—[c]	0.01	—[c]		
	H-6	3.83	—[c]	0.012	—[c]		
	H-6′	3.88	—[c]	0.008	—[c]		
β-CD	H-1	5.08	0.959			0.02	0.93
	H-2	3.66	1.54			0.08	1.53
	H-3	3.98	1.7			0.1	—[c]
	H-4	3.59	0.926			0.01	0.91
	H-5	3.87	—[c]			0.19	0.88
	H-6	3.89	—[c]			0.01	—[c]
	H-6′	3.89	—[c]			0.01	—[c]

[a] $\Delta\delta = \delta_{free} - \delta_{observed}$.
[b] Error in the ^{1}H T_1 values is estimated to be ±5%.
[c] Undetermined value owing to severe overlap of signals.

Table 1 shows also proton T_1 values measured for pure and equimolar mixed solutions of the examined host and guest compounds. The co-presence of both host and guest in solution strongly affects the relaxation rates. This is in line with the observation of the formation of an inclusion complex in solution, although the measured values are weighted averages of the corresponding terms due to all possible supramolecular edifices (including the superimposed motion of the overall molecular motion of the whole complex and the internal motions of the guest in the host cavity) and the great in the free form still present in solution.

In both cases, the average stoichiometry of the complexes in solution was 1:1 (guest:host), as estimated by the Job plot method.[16] Therefore, a binary structure formed by one cyclodextrin molecule surrounding the guest can be considered reliable for both the complexes. The most powerful approach for revealing intermolecular dipolar interactions between the partners in such a supramolecular assembly can be derived by ^1H–^1H NOE NMR experiments. Unfortunately, the inherently small NOE values due to the unfavourable correlation time of cyclodextrin complexes in water solution clearly constitutes a handicap in studying the mutual geometric relationships of this kind of structure. The problem can be overcome, however, by using the rotating-frame NOE experiments (ROESY). In order to avoid the risk of artefacts and mistakes which are currently observed when applying the standard pulse sequence, the most useful T-ROESY experiment was utilized. Genuine intermolecular ROE cross-peaks are shown in the T-ROESY 2D map (Figs 2 and 3).

Inspection of the T-ROESY map relative to the α-CD–CI-844 complex (Fig. 2) allows us to establish a spatial proximity between the phenyl hydrogens of the guest and the H-3 inner protons of the α-CD. A very weak contact between the *meta* hydrogens H-8,10 of the guest and H-5 of the host was also evidenced along with weak dipolar correlations between the same host protons and H-7,11 and H-9 hydrogens of the drug. The absence of any other ROE contact suggests that, in this case, the restricted space available in the host cavity does not allow the guest to be deeply sequestered and the pyridine ring remains preferentially in contact with the surrounding solvent.

Regarding the β-CD complex with CI-844, the 2D contour map (Fig. 3) shows that all the phenyl aromatic protons establish dipolar contacts with the cyclodextrin protons located on the internal wall of the torus and, probably, with the methylenic H-6, whose resonance

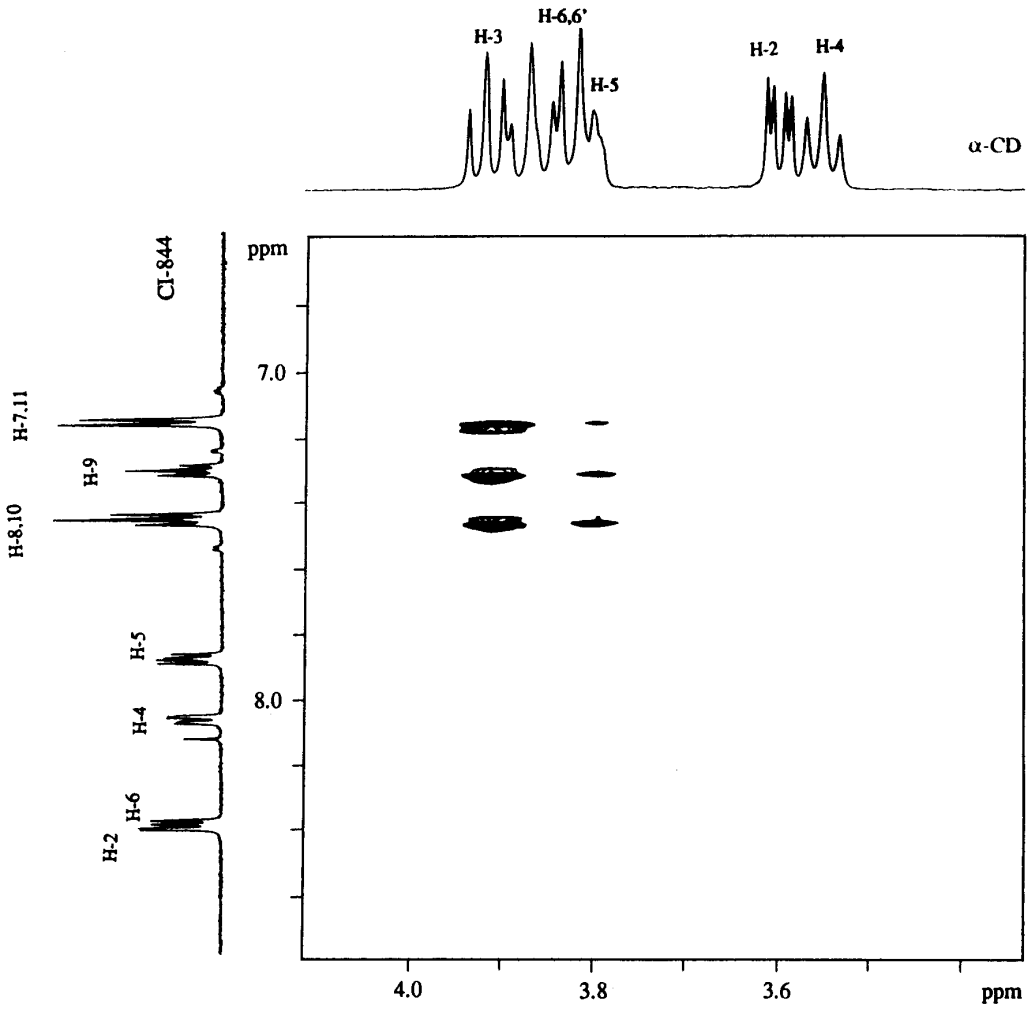

Figure 2. Partial T-ROESY contour plot of equimolecular mixture of α-CD and CI-844.

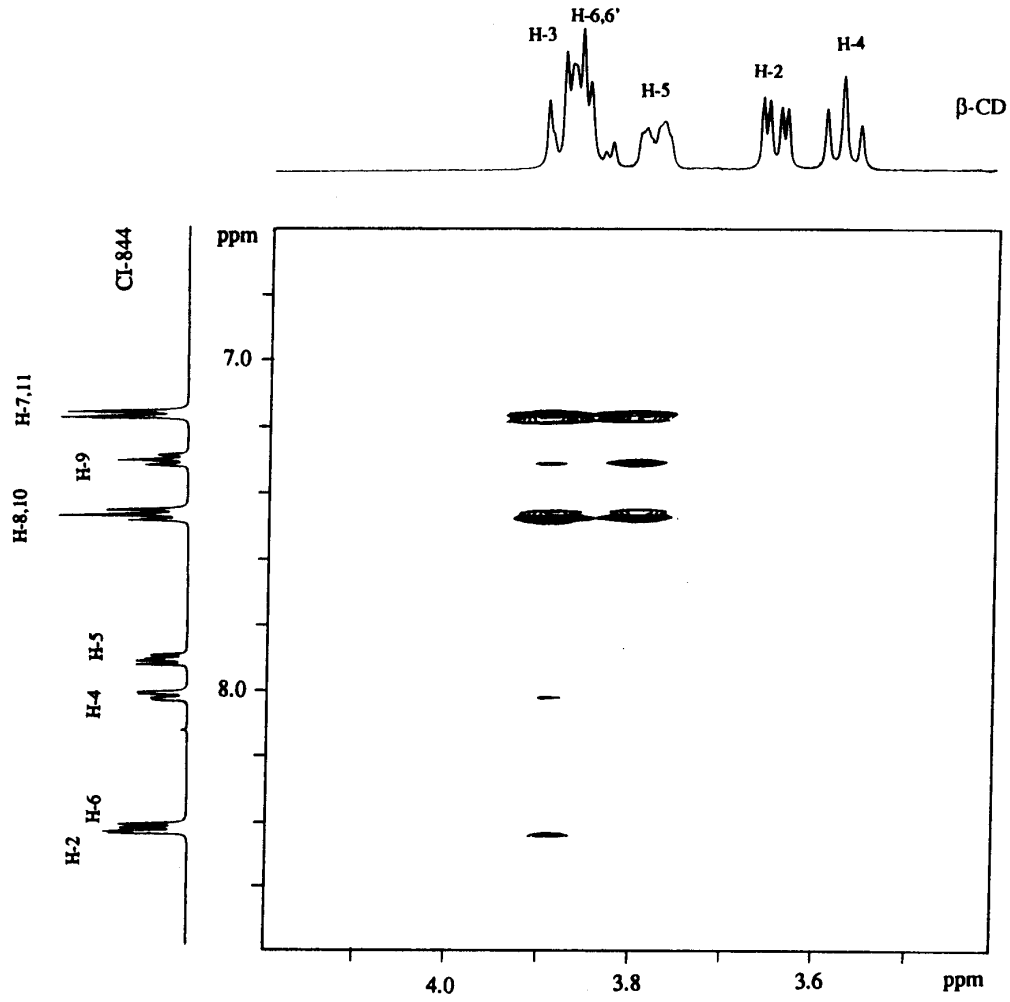

Figure 3. Partial T-ROESY contour plot of equimolecular mixture of β-CD and CI-844.

signals are overlapped with the H-3 signal in the spectrum. The cross peak produced by dipolar coupling between the proton H-9 of the guest and the H-3 hydrogens of the host is significantly weaker than the other cross peak relative to contacts arising from hydrogens of the same phenyl ring. Two weak cross peaks are also detectable in the map attributable to short distance interactions between proton H-2 and H-4 of the guest and the H-3 proton of β-CD.

These data support the hypothesis that the phenyl ring of CI-844 penetrates deeply into the host cavity and that the preferred geometrical disposition could be that depicted in Fig. 4 according to the relative orientation **I** which favours the formation of hydrogen bonds between the guest ether oxygen and host secondary hydroxyl groups.

The above results are also well in line with the measured formation constants (740 and 930 mol^{-1} at 300 K for α- and β-CD complexes, respectively).

Molecular dynamics

An observed NMR ROESY cross peak arises from two hydrogens which are within the dipolar contact distance.[28] Accordingly, predicted cross peaks were determined by analysing the MD simulation trajectories in terms of interatomic hydrogen–hydrogen distances by monitoring every pair of hydrogens which spend most of the simulation time at a distance within the range 0–3.5 Å (assumed limit of dipolar interaction).

In Tables 2 and 3 are listed the pairs of hydrogens that during the simulation time period attained the dipolar contact distance. These values are compared with the intermolecular NMR ROESY correlated hydrogens of the α- and β-CD complexes, respectively.

The gas-phase trajectories of both complexes in the **I** and **II** orientations were initiated from starting structures in which $d = 0.0$ Å. As shown in the tables, those runs did not reproduce the experimental set of contacts. Additional runs were made using starting structures in which the guest was placed at the smaller and at the larger rims by shifting the guest CM by $d = 10$ Å and -10 Å, respectively (Fig. 1). These gas-phase simulations which used modified starting structures also failed. When $d = -10.0$ Å, the simulations of the α-CD complex in both orientations **I** and **II** gave similar sets of contact distances (Table 2). The reason for this is that the complex oriented as **II** with $d = -10.0$ Å evolved towards the structure of the regioisomeric complex **I** also with $d = -10.0$ Å. In the case of the simulations of the β-CD complex ($d = 10.0$ Å starting structures) ana-

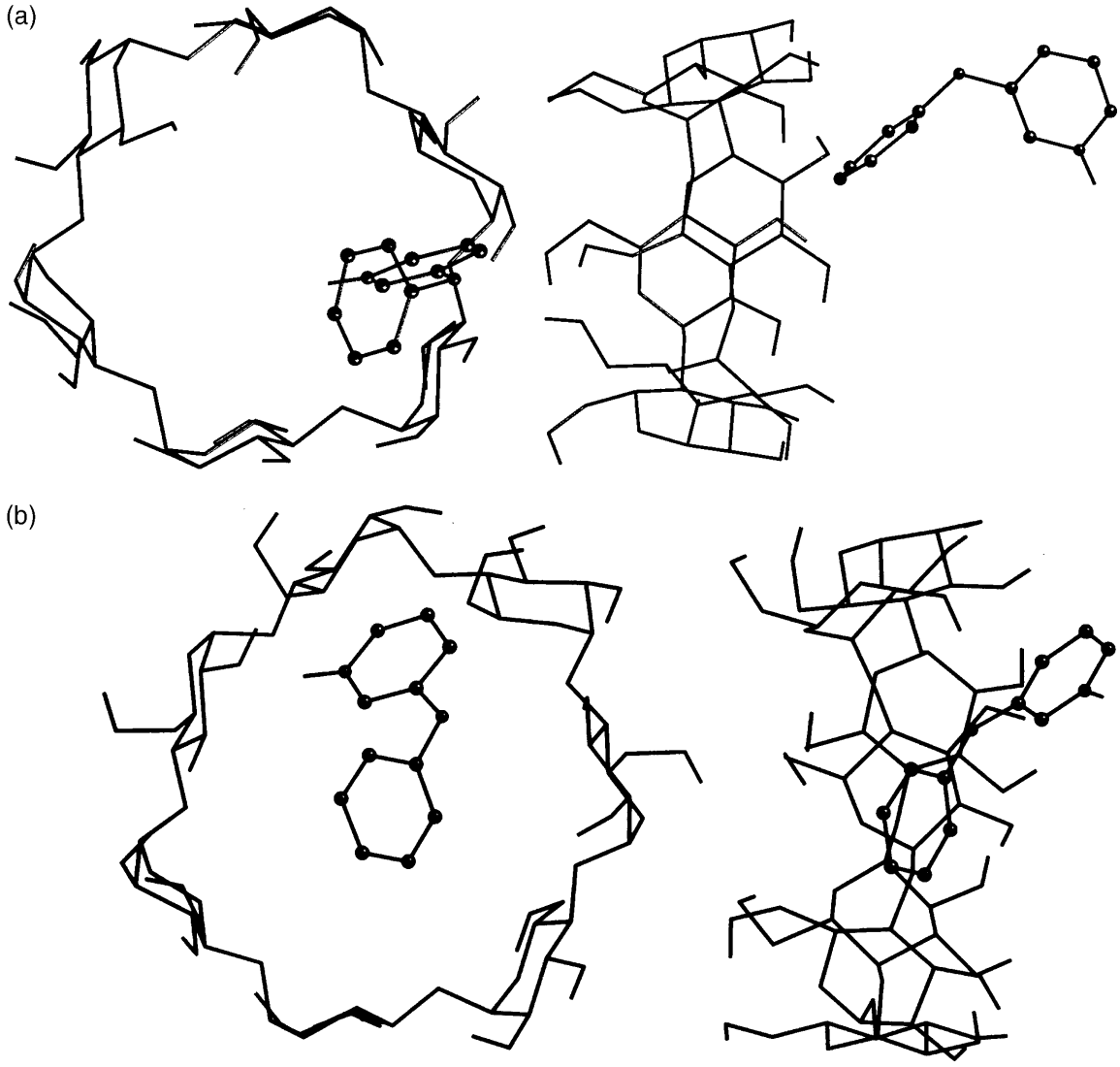

Figure 4. Two projections (orthogonal and parallel to the CDs rims) of the structures and binding geometries of the (a) α-CD and (b) β-CD complexes with CI-844 as attained by snapshots from the MD simulations which reproduced the NMR data sets. To simplify the drawing the surrounding solvent molecules and hydrogen atoms (excluding H-bonded to the oxygens of CDs and to the nitrogen of CI-844) were omitted.

logous reorientation occurred in an inverse fashion, from orientation **I** to **II** (Table 3). The simulations of α- and β-CD complexes using starting structures with $d = 10.0$ Å gave sets of contacts completely inconsistent with the experimental ones (Tables 2 and 3).

However, the simulations of α-CD oriented as **I** with $d = -10.0$ Å and for β-CD oriented as **I** with $d = -10.0$ Å and 0.0 Å provided a number of contacts in agreement with the NMR experiments. From this one may anticipate that both α- and β-CD complexes adopt orientation **I** with the phenoxy ring of the guest facing the larger rim.

The simulations considering explicitly the solvent molecules attained selective agreement between calculated and experimental sets of contacts for both α- and β-CD complexes (Fig. 4). In particular, in the case of the β-CD complex the simulations of the two starting structures at $d = 0.0$ Å gave a set of contacts in agreement with experiment for the host–guest alignment **I** (Table 3). Figure 5(b) shows the migratory aptitude of the guest moving through the annulus of the CD. In this complex the distance between the CMs between the host and the guest fluctuates widely and thus during the simulation time period structures at $d \neq 0.0$ can be easily accessible. For this reason, and on the basis of the results from the gas-phase simulations, trials using starting structures having d values other than 0.0 Å were unnecessary.

The simulation of the α-CD complex with host and guest oriented as **I** and with $d = -7.5$ Å resulted in good agreement with experiment (Table 2) (the choice of the value $d = -7.5$ Å in place of $d = -10.0$ Å in the liquid-phase model was due to the size of the water sphere used) Analysis of the trajectory [Fig. 5(a)] indicated that during its evolution the guest fluctuates widely but does not penetrate deeply into the cavity. The results of the simulations of the complex with the CMs initially coincident are analogous to those obtained in the gas phase, i.e. lack of agreement between the sets of contacts, guest molecule constrained

Table 2. NMR T-ROESY cross peaks (marked by ⊗) between α-CD and CI-844 hydrogens determined for the complex in D_2O, and theoretical cross peaks produced by MD simulations (marked by ○ and □ for the relative host–guest orientations denoted by **I** and **II**, respectively)[a]

			MD simulations									
			Gas phase						Liquid phase			
Hydrogens			$d = 0.0$ Å		$d = -10.0$ Å		$d = 10.0$ Å		$d = 0.0$ Å		$d = -7.5$ Å	
α-CD	CI-844	NMR	**I**	**II**	**I**	**II**	**I**	**II**	**I**	**II**	**I**	**II**
H-3	H-2		○	□	○	□			○			□
H-3	H-4		○						○	□		
H-3	H-5								○			
H-3	H-6											
H-3	H-7,11	⊗	○	□	○	□			○	□	○	
H-3	H-9	⊗		□	○	□				□	○	
H-3	H-8,10	⊗		□	○	□				□	○	
H-5	H-2		○	□			○		○	□		
H-5	H-4			□			○		○	□		
H-5	H-5						○	□		□		
H-5	H-6						○	□				
H-5	H-7,11	⊗[b]	○						○	□		
H-5	H-9	⊗[b]	○		○	□					○	
H-5	H-8,10	⊗	○		○	□			○	□	○	
H-6	H-2			□			○	□		□		
H-6	H-4			□			○	□		□		
H-6	H-5						○	□		□		
H-6	H-6						○	□				
H-6	H-7,11		○				○		○	□		
H-6	H-9		○						○			
H-6	H-8,10		○				○		○			

[a] The MD calculated cross peaks represent the pairs of intermolecular hydrogen atoms that fluctuate at the NOE effective distance (≤3.5 Å). The *d* values (Å) represent the distances between the CMs of the host and guest in the starting structures.
[b] Very weak cross peaks (Fig. 2).

inside the host's cavity and very restricted fluctuations of the CMs distance (Fig. 6). This confirms the gas-phase predictions of a bottle-neck type energy barrier due to the small dimensions of the α-CD torus preventing the guest from moving freely from one side of the CD to the other through the macrocycle interior.

Features of the simulation of the **II** oriented α-CD complex with $d = -7.5$ Å are a single ^1H–^1H contact, which is not observed among the experimental ones, and a proclivity of the guest to diffuse far away from the host. In a single run among the repeated simulations of the α-CD complex oriented as **I** with CM origins shifted by $d = -7.5$ Å, the complex dissociates after a certain evolution time. This is in agreement with the observed smaller NMR upfield shifts of the inner α-CD hydrogens resonances with respect to the corresponding ones of β-CD.

In Tables 4 and 5 we report the averaged values of the total potential energies and component energies for all the trajectories described above. The energy values in the liquid were attained by post-processing of the trajectories, by considering only the atoms of the solute and using, for consistency, the same dielectric constant as used in the gas-phase simulations. The tables also report the energies of the non-complexed species (NC) obtained from separate MD simulations of each single host and guest molecule in the gas and liquid phases.

In general, the complexes in both the gas and liquid phases attained lower energies than the NC species in their respective phase. The only exception to this is for the liquid-phase α-CD complex in the **II** orientation starting at $d = -7.5$ Å. Thus the CHARMm force-field MD simulations predict that CI-844 forms complexes with CDs that are energetically stable. However, it also predicts that complexes oriented as **II** should be more stable than those oriented as **I**; in fact, as a general trend, from Tables 4 and 5 in nearly all the simulations the **II** orientation has a lower energy than the **I** orientation. This is not in agreement with the above analysis of the NMR T-ROESY contacts, which indicate that both α- and β-CD complexes stay in the **I** orientation.

To account for this finding, we extracted from the separate simulation of CI-844 in water the interaction energies of the phenyl and the pyridinium moieties with all the H_2O molecules (448) contained in the simulation sphere. The data presented in Table 6 show that the water molecules are much more tightly bonded to the pyridinium ring than to the phenyl ring. This implies that depletion of solvent molecules from the hydration sphere of the phenyl moiety occurs more easily than

Table 3. NMR T-ROESY cross peaks (marked by ⊗) between β-CD and CI-844 hydrogens determined for the complex in D_2O, and theoretical cross peaks produced by MD simulations (marked by ○ and □ for the relative host–guest orientations denoted by I and II, respectively)[a]

			MD simulations							
			Gas phase						Liquid phase	
Hydrogens			$d = 0.0$ Å		$d = -10.0$ Å		$d = 10.0$ Å		$d = 0.0$ Å	
β-CD	CI-844	NMR	I	II	I	II	I	II	I	II
H-3	H-2	⊗	○		○				○	
H-3	H-4	⊗	○		○				○	
H-3	H-5									
H-3	H-6									
H-3	H-7,11	⊗	○	□	○	□	○	□	○	□
H-3	H-9	⊗		□		□	○	□	○	□
H-3	H-8,10	⊗	○	□		□	○	□	○	□
H-5	H-2		○	□	○	□	○	□		□
H-5	H-4			□		□	○	□		□
H-5	H-5									
H-5	H-6									
H-5	H-7,11	⊗	○	□	○	□	○	□	○	□
H-5	H-9	⊗	○						○	□
H-5	H-8,10	⊗	○	□	○	□	○	□	○	□
H-6	H-2			□		□	○	□		□
H-6	H-4			□		□	○	□		□
H-6	H-5			□						
H-6	H-6			□						
H-6	H-7,11		○	□	○					□
H-6	H-9	×[b]	○		○				○	
H-6	H-8,10	×[b]	○		○				○	

[a] The MD calculated cross peaks represent the pairs of intermolecular hydrogen atoms that fluctuate at the NOE effective distance (⩽3.5 Å). The d values (Å) represent the distances between the CMs of the host and guest in the starting structures.
[b] Signals overlapped with H-3 resonances of the β-CD.

from the hydration sphere of the pyridinium ring. Consequently, if one considers the solvent's effects during the complexation, it can be argued that the type **I** orientation together with inserting the guest's phenyl ring through the hydrophobic cavity of the host should be favoured.

From Tables 4 and 5, useful trends can be found which highlight the factors responsible for the differences obtained from the gas- and liquid-phase MD simulations in the systems dealt with here. The differential energies between the gas- and liquid-phase simulations indicate that the NC species, and even the complexed systems, have higher energy in the liquid. For the α-CD–CI-844 NC species the differences is 16.12 kcal mol^{-1}, whereas for the β-CD–CI-844 NC species it is 15.24 kcal mol^{-1}. Relevant contributions to the increased total energies in the liquid phase originate from the electrostatic and H-bond terms. Further, the tables show that in the gas-phase simulations *all* the non-bond interactions (i.e. van der Waals, electrostatic and H-bond) contribute to the formation and stabilization of the complexes. In contrast, in the liquid phase the driving force is almost exclusively due to the van der Waals interaction.

This indicates that the failure of the gas-phase models can be attributed to an overestimation of the electrostatic and H-bond terms due to the absence of explicit water molecules surrounding the solute.

CONCLUSIONS

We have studied the binding of a nootropic drug, CI-844, to macrocyclic host molecules having potential as delivery vehicles. We have presented detailed NMR data concerning the mode of drug binding to two CDs in aqueous solution. Complementing this is an assessment of MD protocols commonly used to help interpret such NMR data.

From our NMR studies we found the following: (i) CI-844 forms inclusion complexes with α- and β-CD, with a 1:1 stoichiometry; (ii) the phenyl ring gives dipolar contacts between all its protons and the inner, H-3 and H-5, protons of both α- and β-CD host molecules; (iii) the pyridinium moiety has only two protons giving dipolar contacts with just β-CD inner protons; (iv) α-CD inner protons have smaller upfield shifts than the β-CD inner protons. Generally, we note that NMR data are not capable of giving directly detailed insights

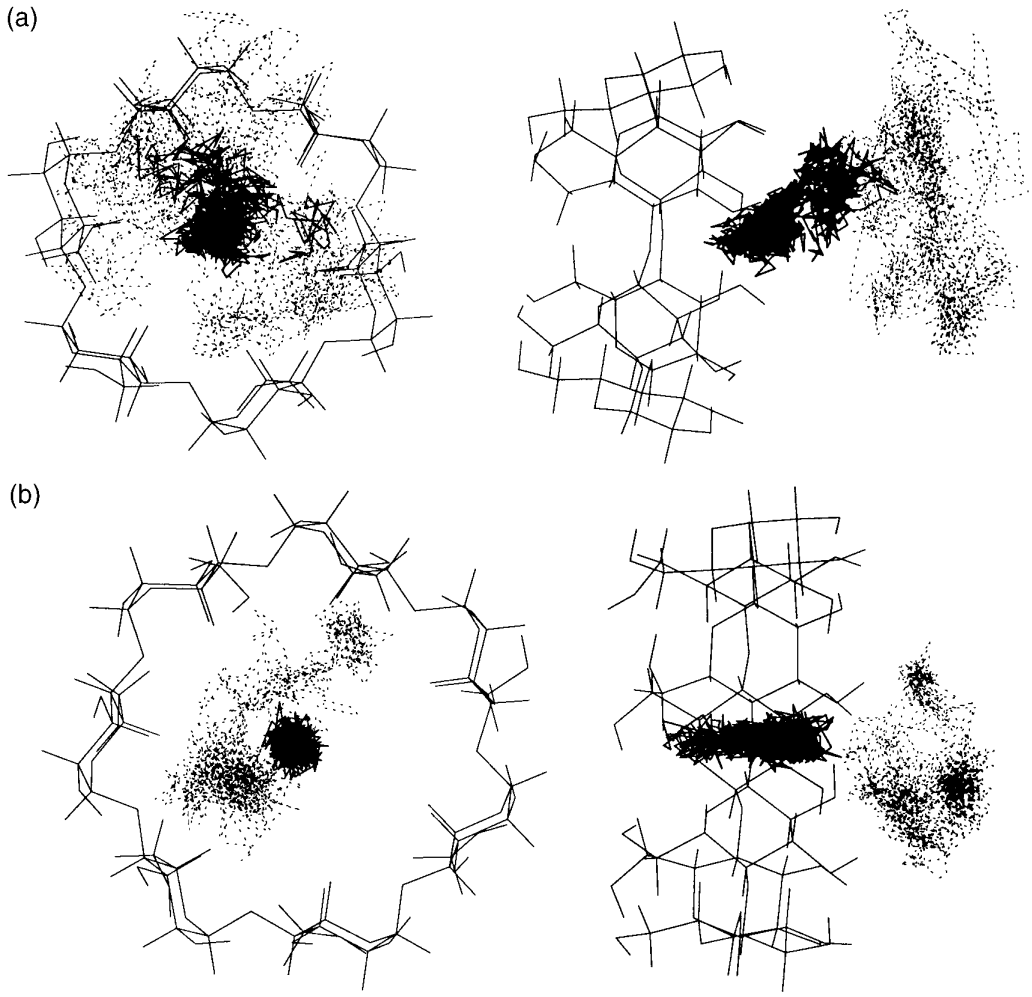

Figure 5. Fluctuations from MD simulations in liquid of the guest with respect to a fixed host reference system in the (a) α-CD and (b) β-CD complexes. The solid and the dotted lines refer to the positions attained during the simulations by the centres of the phenyl and pyridinium moieties, respectively, of CI-844. The simulations refer to the complexes in the **I** orientation and to the starting structures at $d = -7.5$ and 0.0 Å for α-CD and β-CD complexes, respectively.

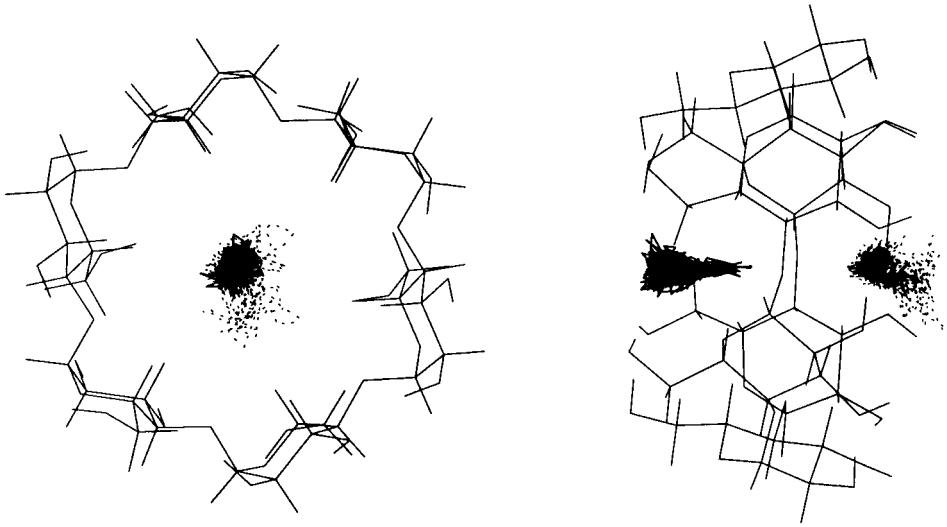

Figure 6. Fluctuations from MD simulations in liquid of the guest with respect to a fixed host reference system in the α-CD complex. The solid and the dotted lines refer to the positions attained during the simulations by the centres of the phenyl and pyridinium moieties, respectively, of CI-844. The simulation refers to the complex in the **I** orientation with starting structure at $d = 0.0$ Å.

Table 4. Averaged total energies and contributing terms (kcal mol^{-1}) calculated from the gas- and liquid-phase MD trajectories of the α-CD–CI-844 complex at the various starting structures and host–guest relative alignments, and of the host and guest as non-complexed (NC) species[a]

	Gas phase							Liquid phase				
	$d = 0.0$ Å		$d = -10.0$ Å		$d = 10.0$ Å			$d = 0.0$ Å		$d = -7.5$ Å		
Energy	I	II	I	II	I	II	NC	I	II	I	II	NC
Total	130.15	112.44	119.61	120.30	128.33	127.31	148.36	141.35	134.51	154.68	167.08	164.48
Bond	28.84	28.64	28.16	27.91	28.18	28.33	27.96	27.87	27.75	27.77	31.41	27.54
Angle	84.49	86.20	82.85	81.51	83.61	84.22	81.62	81.67	82.63	81.37	90.12	80.93
Dihedral	152.17	149.96	149.05	151.17	152.66	152.91	154.33	150.10	148.65	150.01	174.22	148.89
Improper	2.44	2.46	2.33	2.22	2.43	2.39	2.38	2.39	2.40	2.42	2.22	2.29
Van der Waals	−32.97	−36.71	−23.54	−22.77	−20.90	−20.62	−14.03	−39.09	−38.75	−29.46	−23.79	−18.71
Electrostatic	−79.49	−79.60	−84.38	−92.88	−86.71	−87.17	−79.17	−59.69	−65.43	−55.28	−80.55	−55.56
H-bond	−25.33	−38.51	−34.87	−26.87	−30.95	−32.77	−24.73	−21.89	−22.75	−22.16	−26.57	−20.95

[a] The energies in the liquid were calculated considering only the solute–solute interactions and using a distance-dependent dielectric constant.

Table 5. Averaged total energies and contributing terms (kcal mol^{-1}) calculated from the gas- and liquid-phase MD trajectories of the β-CD–CI-844 complex at the various starting structures and host–guest relative alignments, and of the host and guest as non-complexed (NC) species[a]

	Gas phase							Liquid phase		
	$d = 0.0$ Å		$d = -10.0$ Å		$d = 10.0$ Å			$d = 0.0$ Å		
Energy	I	II	I	II	I	II	NC	I	II	NC
Total	127.18	121.66	131.27	115.60	116.67	116.67	156.42	160.59	148.79	171.66
Bond	33.76	33.23	31.99	32.24	31.96	31.96	33.24	38.15	38.27	31.18
Angle	95.23	92.89	93.59	95.40	94.77	94.77	92.74	91.94	91.89	90.38
Dihedral	177.22	174.83	176.55	175.46	176.00	176.00	177.95	174.30	172.94	174.83
Improper	2.44	2.36	2.19	2.35	2.34	2.34	2.38	2.46	2.50	2.29
Van der Waals	−33.85	−34.70	−33.72	−33.99	−33.34	−33.34	−15.78	−38.36	−38.17	−20.67
Electrostatic	−106.88	−110.84	−101.23	−109.56	−108.52	−108.52	−99.83	−82.20	−92.73	−81.27
H-bond	−40.73	−36.10	−38.11	−46.31	−46.53	−46.53	−34.28	−25.69	−25.89	−25.13

[a] The energies in the liquid were calculated considering only the solute–solute interactions and using a distance-dependent dielectric constant.

into supramolecular structure. However, in this particular case, since the guest molecule has a very simple geometry, it was possible to determine that both complexes of CI-844 with α- or β-CD have type **I** orientation with the phenyl ring inserted in the cavity from the larger rim side.

From our MD simulations we found the following: (i) the complexes are energetically stable; (ii) each complex assumes type **I** orientation with the phenyl ring facing the larger rim for α-CD and deeply nested inside the cavity from the larger rim side for β-CD; (iii) in both complexes the guest molecule's CM fluctuates widely; (iv) the relative hydrophilic–hydrophobic features of the two ring moieties of the guest molecule are responsible for determining the guest orientation of the included complexes.

To obtain these results, simulations with explicit water molecules were needed. The gas-phase simulations evidenced lack of consistency with the NMR dipolar contacts, giving only a first rough indication of the structure of each complex. The reason for this failure was found to be due to an overestimation of the electrostatic and H-bond terms, which are improperly treated in ionic species.

Further, this study has evidenced, from a methodological point of view, the importance of sampling a wide portion of the system's phase space by implementing many runs with different starting conditions (i.e. various structural configurations of the complex). It also indicates that when studying a system that requires explicit water (or solvent) molecules included in the model, preliminary gas-phase simulations can be exploited by restricting the costly water simulations to a limited set using starting structures selected from those gas-phase simulations having the most meaningful results compared with experiments. Hence a computational protocol that simplifies the numerical work in performing MD simulations of solvated host–guest complexes is possible when making comparisons with NMR data.

Finally, the study indicated that the β-CD is more suited than the α-CD for the vehiculation of CI-844.

Table 6. Averaged interaction energies (kcal mol^{-1}) of the phenyl and pyridinium fragments of CI-844 with water, calculated from MD trajectory of CI-844 immersed in 448 water molecules

Energy	Phenyl	Pyridinium
Total	−22.59	−84.07
Van der Waals	−12.62	−10.85
Electrostatic	−9.97	−73.22

Acknowledgement

Thanks are due to Parke-Davis Werner-Lambert (Dr Carol Germain) for the kind gift of the sample of CI-844.

REFERENCES

1. D. Duchêne, *New Trends in Cyclodextrins and Derivatives*. Editions de Santé, Paris (1991).
2. J. Szejtli, *Cyclodextrin Technology*. Kluwer, Dordrecht (1988).
3. K. A. Connors, *Chem. Rev.* **97**, 1325 (1997).
4. K. Uekama and M. Otahiri, *CRC Crit. Rev. Ther. Drug Carrier Syst.* **3** (2), 1 (1991).
5. P. Tallal, *J. Clin. Psychopharmacol.* **5**, 272 (1985).
6. J. Kabes, *J. Int. Med. Chem. Res.* **13**, 185 (1985).
7. D. E. Butler, P. Bass, I. C. Nardin, F. P. Hauck, Jr, and Y. J. L'Italien, *J. Med. Chem.* **14**, 575 (1971).
8. D. E. Butler, B. P. H. Poschel and J. G. Marriott, *J. Med. Chem.* **24**, 346 (1981).
9. K. B. Lipkowitz, *Chem. Rev.*, **98**, 1829 (1998), and references cited therein.
10. F. Djedaini and B. Perly, in *New Trends in Cyclodextrins and Derivatives*, Editions de Santé, Paris, 1991, pp. 217–246.
11. M. E. Amato, G. C. Pappalardo and B. Perly, *Magn. Reson. Chem.* **31**, 455 (1993).
12. M. E. Amato, G. M. Lombardo, G. C. Pappalardo and G. Scarlata, *J. Mol. Struct.* **350**, 71 (1995).
13. M. P. Allen and D. J. Tildesley, *Computer Simulations of Liquids*. Clarendon Press, Oxford (1987).
14. W. F. Van Gunsteren, P. K. Weiner and A. J. Wilkinson (Eds) *Computer Simulation of Biomolecular Systems: Theoretical and Experimental Applications*, Vol. 2. ESCOM Science Publishers Leiden (1993).
15. M. E. Amato, K. B. Lipkowitz, G. M. Lombardo and G. C. Pappalardo, *J. Chem. Soc., Perkin Trans. 2* 321 (1996).

16. P. Job, *Ann. Chim.* **9**, 113 (1928).
17. H. A. Benesi and J. A. Hildebrand, *J. Am. Chem. Soc.* **71**, 2703 (1949).
18. T.-L. Hwang and A. J. Shaka, *J. Am. Chem. Soc.*, **114**, 3157 (1992); *J. Magn. Reson.* **102**, 155 (1993).
19. M. L. Martin, G. J. Martin and J.-J. Delpeuch, *Practical NMR Spectroscopy*. Heyden, London (1980).
20. B. R. Brooks, R. E. Bruccoleri, B. D. Olafson, D. J. States, S. Swaminathan and M. Karplus, *J. Comput. Chem.* **4**, 187 (1983).
21. G. Bandoli, A. Grassi, E. Montoneri, G. C. Pappalardo and B. Perly, *J. Mol. Struct.* **172**, 369 (1988).
22. K. K. Chacko and W. Saenger, *J. Am. Chem. Soc.* **103**, 1708 (1981).
23. K. Lindner and W. Saenger, *Carbohydr. Res.* **99**, 103 (1982).
24. H. Harata, *Bull. Chem. Soc. Jpn.* **61**, 1939 (1988).
25. B. H. Bessler, K. M. Merz, Jr, and P. A. Kollman, *J. Comput. Chem.* **11**, 431 (1990).
26. J. J. P. Stewart, *MOPAC-6, QCPE 455* (1990).
27. C. L. Brooks III and M. Karplus, *J. Chem. Phys.* **79**, 6312 (1983).
28. D. Neuhaus and M. P. Williamson, *The Nuclear Overhauser Effect in Structural and Conformational Analysis*. VCH, New York (1989).

